

CoreGuard: Safeguarding Foundational Capabilities of LLMs Against Model Stealing in Edge Deployment

Qinfeng Li
Zhejiang University
Hangzhou, China

Zhiqiang Shen
Zhejiang University
Hangzhou, China

Xinkui Zhao
Zhejiang University
Hangzhou, China

Yangfan Xie
Zhejiang University
Hangzhou, China

Zhengan Qin
Zhejiang University
Hangzhou, China

XianWei Zhu
China Electronics Technology Design
and Research Institute
Beijing, China

Xuhong Zhang*
Zhejiang University
Hangzhou, China

Tianyu Du
Zhejiang University
Hangzhou, China

Hao Peng
Zhejiang Normal University
Jinhua, China

Jianwei Yin
Zhejiang University
Hangzhou, China

ABSTRACT

Proprietary large language models (LLMs) demonstrate exceptional generalization ability across various tasks. Additionally, deploying LLMs on edge devices is trending for efficiency and privacy reasons. However, edge deployment of proprietary LLMs introduces new security threats: attackers who obtain an edge-deployed LLM can easily use it as a base model for various tasks due to its high generalization ability, which we call foundational capability stealing. Unfortunately, existing model protection mechanisms are often task-specific and fail to protect general-purpose LLMs, as they mainly focus on protecting task-related parameters using trusted execution environments (TEEs). Although some recent TEE-based methods are able to protect the overall model parameters in a computation-efficient way, they still suffer from prohibitive communication costs between TEE and CPU/GPU, making it impractical to deploy for edge LLMs. To protect the foundational capabilities of edge LLMs, we propose CoreGuard, a computation- and communication-efficient model protection approach against model stealing on edge devices. The core component of CoreGuard is a lightweight and propagative authorization module residing in TEE. Extensive experiments show that CoreGuard achieves the same security protection as the black-box security guarantees with negligible overhead.

KEYWORDS

Intellectual Property Protection, Edge-deployed Transformer Model, Authorization, Trusted Execution Environment

1 INTRODUCTION

Large language models (LLMs), especially proprietary ones such as ChatGPT [10] and Claude [25], demonstrate exceptional generalization ability across various tasks [4, 28]. Additionally, deploying

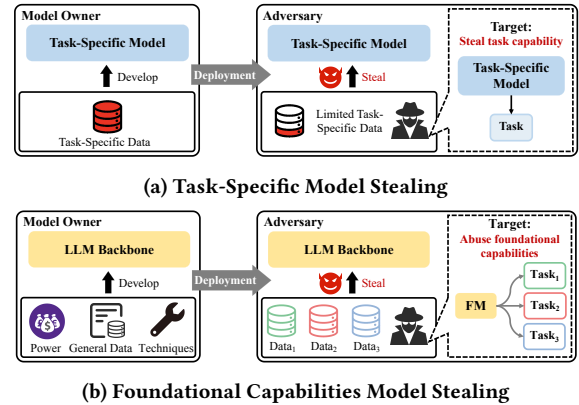


Figure 1: Paradigms of model stealing. (a) Task-specific model stealing: the adversary steals the task capability of the model. (b) Foundational capabilities model stealing: the adversary abuses the backbone for various tasks with abundant data.

LLMs on edge devices is a growing trend for latency- and privacy-sensitive tasks, e.g., Apple Inc. introduced Apple Intelligence, which integrates a 3-billion-parameter LLM into users' devices in the latest iOS version [3]. To protect edge-deployed models from stealing, many methods [33, 44] have been proposed. However, these methods are mainly designed for task-specific models, while for general-purpose LLMs, their edge deployment introduces new security: attackers who obtain an edge-deployed LLM can easily use it as a base model for various tasks due to its high generalization ability. We refer to this kind of theft as *foundational capability stealing*. Leakage of foundational capabilities can lead to significant harm to model owners, including substantial financial losses, the erosion of technological advantage, etc. Therefore, preventing edge-deployed LLMs from unauthorized usage is crucial.

*Corresponding author

Unfortunately, existing model protection solutions [22, 31, 44] can hardly be applied to protect the foundational capabilities of LLMs, as traditionally deployed models are mostly task-specific, whose threat is inherently different from that of LLMs (as shown in Figure 1). Specifically, a task-specific model is usually trained from scratch or fine-tuned on a pre-trained model with a task-specific dataset, which is typically proprietary to the model owner. In this case, the scarcity of the task-specific dataset is the primary barrier for others to replicate this model, which is why most model-stealing methods [26, 27] usually assume the attacker possesses limited (e.g., 1%) task-specific data. Consequently, task-specific stealing is fundamentally data-oriented stealing. However, with the emergence of LLMs, its foundational capabilities have become a new scarce resource, making it a new target for stealing. Specifically, proprietary LLMs, like GPT-4, developed with prohibitive costs, can serve as exceptional backbones for various tasks. However, access to these models usually involves considerable financial costs to users. Therefore, to achieve good performance on various tasks without financial cost, foundational capability stealing becomes attractive. In this way, attackers could use the backbone on various tasks, where they might have plenty of data. Therefore, securing backbones demands effective protection across various tasks faced with sufficient training data, while protecting task-specific models only requires safeguarding a single task against limited data. Essentially, for task-specific models, the task-related parameters present the most valuable components, while for LLMs, all parameters must be protected. Therefore, existing task-specific solutions fail to protect the LLMs. For instance, Zhang et al. [44] protect task-specific parameters within a Trusted Execution Environment (TEE), which is an isolated hardware enclave that securely stores and executes sensitive data, but leaves the backbone unprotected, exposing its foundational capabilities to be misused.

To protect the backbone, a straightforward idea is to place the entire model in the TEE. However, straightforward black-box protection by TEEs is impractical because shielding entire LLMs within TEEs results in a roughly 50× reduction in model execution efficiency due to TEEs’ limited computational speed [37]. To reduce TEE execution overhead, some researchers [22, 31] propose only placing a subset of the model (e.g., the last layer) in TEEs and offloading the rest of the computation to GPUs, i.e., Partial Parameter TEE Execution (PPTE). However, prior work [44] proves that PPTE even fails to protect task-specific models due to an unresolved balance between model security and TEE execution overhead. Essentially, PPTEs crudely load the sensitive parameters into TEE for protection, where the limited computational power of TEEs restricts the number of protected parameters, thus compromising security.

To increase the number of protected parameters, a promising approach is to protect parameters through shuffling, i.e., Parameter Shuffling Protection (PSP) [18, 33]. For example, ShadowNet [33] proposes executing all linear transformation layers (e.g., convolutional and linear layers) on the GPU. To secure these GPU-executed parameters, ShadowNet shuffles the channels of the convolutional kernels, ensuring that only the corresponding shuffled feature maps can be correctly computed with these shuffled parameters. This feature map shuffling process is performed within the TEE thus ensuring its security. However, the excessive data transfer overhead

between the TEE and GPU makes this protection infeasible for edge-deployed LLMs. Specifically, before every linear layer, the features must be transferred from the GPU to the TEE and then back to the GPU. For example, consider a float-32 LLaMA3-8B model, which contains 224 linear layers. Using ShadowNet to protect this model would result in 448 TEE-CPU transfers to generate a single token (each linear layer requires 2 transfers). Therefore, with an input length of 128 context length, each transfer would average 3MB of data, leading to a total data transfer volume of approximately 1.3GB (448 × 3MB). Given that mainstream mobile platform TEEs, like TrustZone, have a data transfer rate of about 1GB/s between the TEE and CPU [2], the time to generate a single token would be approximately 1.3 seconds. Consequently, producing a complete output would require several hundred seconds (assuming it consists of 100 tokens) solely for data transfer between the TEE and CPU, even before accounting for additional CPU-GPU transfer time.

In summary, existing solutions suffer from unacceptable computation or communication overhead. To protect the foundational capabilities of edge-deployed LLMs, we propose a computation- and communication-efficient model protection approach, CoreGuard. To reduce TEE execution overhead, CoreGuard is inspired by prior PSP solutions by executing all model computations on the GPU and securing GPU-executed parameters with a permutation strategy. Specifically, CoreGuard utilizes a *protection protocol*, which row-permutes the weight matrix of linear layers, ensuring their input features must be correspondingly column-permuted (i.e., authorization) by trusted hardware, i.e., TEE. Crucially, to minimize TEE-GPU transfer overhead, CoreGuard introduces a *propagation protocol* that minimizes TEE authorization frequency. Specifically, the propagation protocol column-permutes certain layers so that they can perform column permutations on their own outputs, allowing the subsequent layers to be authorized without the involvement of the TEE. In this way, the TEE only needs to manage the initial authorization, and the authorization can be propagated to all subsequent layers.

Our evaluation shows that CoreGuard outperforms existing defenses in security and efficiency. Attackers can hardly obtain any performance promotion by model stealing (MS) attacks compared to the black-box baseline (i.e., shielding the whole model in TEE). Besides, the experimental results show no difference in accuracy between the CoreGuard-protected model and the original model. The contributions of this work are as follows:

- We are the first to address the protection of foundational capabilities in edge-deployed LLMs. We clearly distinguish between foundational capabilities stealing and traditional task-specific stealing from the perspectives of motivation, targets, and available data.
- We propose CoreGuard, a plug-and-play solution that utilizes a lightweight authorization mechanism to protect edge-deployed LLMs. Notably, this authorization mechanism employs a propagation protocol, significantly reducing transfer overhead while maintaining a low computation overhead.
- Extensive experiments demonstrate that compared to the existing solutions, CoreGuard offers a higher security guarantee with lower overhead and no accuracy loss.

2 BACKGROUND AND THREAT MODEL

2.1 Background

TEE. A Trusted Execution Environment (TEE) is an isolated hardware enclave that stores and processes sensitive data. Popular TEE implementations include Intel SGX [20], AMD SEV [14], and TrustZone [2]. In this paper, we follow prior work [44] and deem TEE a secure area on a potential adversary host device (including GPUs). This means the data, code, and computation processes inside TEEs are secure. Although there are side-channel attacks that may leak sensitive data from TEE, they are out of the scope of this paper.

2.2 Threat Model

In this paper, we consider two parties: the defender and the attacker. The defender is the party that owns the edge-deployed model. The attacker aims to steal the edge-deployed model.

Defender’s Goal. The goal of the defender is to deploy a locked model on the device and ensure that it only works when proper authorization is given by the trusted hardware (i.e., TEE) within the device.

Adversary’s Goal. The attacker aims to abuse the foundational capabilities of the deployed model for their task. A straightforward way to achieve this is trying to reverse the authorization process so that the locked model can be used independently of the device. Another more practical new way is to fine-tune the locked model to obtain a model that excels at a desired task.

Adversary’s Capability. The attacker could *decide the target task*, where they *possess sufficient well-labeled datasets* for the desired task. In this paper, we consider TEE to be a secure world, that cannot be compromised, while other hardware (e.g., GPU and CPU) could be exposed to attackers in a white-box manner. Therefore, the attacker can have white-box access to the details, e.g., model architecture and weights, of the locked model resides outside TEE.

3 DESIGN OF COREGUARD

This section presents our proposed protection method, CoreGuard, which utilizes a permutation strategy to address the key requirements outlined in Section 1.

3.1 Approach Overview

As shown in Figure 2, CoreGuard operates in two phases: model locking (before deployment) and inference authorization (post-deployment).

In the model locking phase, CoreGuard locks a trained model by applying a **protection protocol** to the weights of linear layers, i.e., swapping rows of the weight matrix. These row permutations essentially act as a *lock*, rendering the linear layers dysfunctional, thus making the overall model unusable. These row-permuted layers can only function properly with inputs that are correspondingly column-permuted, which essentially acts as *authorization*. However, authorizing the input features of each permuted layer using the TEE would result in significant TEE-GPU transfer overhead. To address this, CoreGuard proposes a **propagation protocol**, which enables the features to be column-permuted by the network itself. Specifically, CoreGuard permutes the columns of certain layers,

thus through their operation, their output features are column-permuted, which achieve authorization similarly. In this way, the TEE only needs to manage the initial authorization, and the authorization can be propagated to all subsequent layers.

In the inference authorization phase, the TEE manages the initial authorization by applying a column permutation to the input features for authorized use. However, using TEE directly for this column permutation can leave the process vulnerable to input-output speculation (i.e., inferring the permutation order by comparing features before and after the permutation). To avoid this, CoreGuard encrypts the input feature in advance. However, encrypting the features just before they enter the TEE is ineffective, as the attacker can obtain the previous layer’s output, which is unencrypted. Furthermore, placing the encryption process before the previous add-norm layer is still ineffective, as the add-norm layer does not change the relative magnitudes of the elements, allowing the attacker to utilize the unencrypted output feature of the layer before the add-norm layer. Therefore, we place the encryption process before the output linear layer of the FFN block. Specifically, a one-time pad (OTP) encryption is applied, which generates a random mask and adds the mask to the feature for concealment [30]. To further secure this encryption process, we introduce a permutation to obfuscate the masked features and apply a corresponding permutation to the linear layer to prevent this permutation from affecting the computation’s correctness.

3.2 Model Locking

Given a classic transformer layer, we describe how to permute its weights for protection. This permutation first applies the protection protocol to layers involved in input feature projection (e.g., the QKV projection layer in the attention block and the input linear layer in the FFN block) to secure the model. Then, the propagation protocol is applied to layers managing output projection (e.g., the output projection layer in the attention block and the output linear layer in the FFN block) to propagate authorization.

Transformer Layer Formalization. We begin by formalizing a standard transformer layer. Let x , and $z \in \mathbb{R}^{l \times d}$ denote its input and output, where l is the sequence length (e.g., the number of tokens) and d is the model dimension. We define a classic attention block as a function $f_w : \mathbb{R}^{l \times d} \rightarrow \mathbb{R}^{l \times d}$ with weight parameters w . The transformer layer, i.e., $f_w(x) = z$, is computed as follows:

$$\begin{aligned}
 Q &= xW_q, K = xW_k, V = xW_v, && // Q, K, V \text{ projections} \\
 o &= \text{softmax} \left(\frac{QK^T}{\sqrt{d/h}} + M \right) VW_o, && // \text{Attention calculation} \\
 y &= \gamma_1 \odot \frac{o + x - \mu_{o+x}}{\sigma_{o+x}} + \beta_1, && // \text{Add \& norm} \quad (1) \\
 m &= \text{ReLU}(yW_m + b_m), && // \text{FFN input} \\
 n &= mW_n + b_n && // \text{FFN output} \\
 z &= \gamma_2 \odot \frac{y + n - \mu_{y+n}}{\sigma_{y+n}} + \beta_2, && // \text{Add \& norm}
 \end{aligned}$$

where w includes the attention weights W_q, W_k, W_v , and $W_o \in \mathbb{R}^{d \times d}$, the add-norm weights $\gamma_1, \beta_1, \gamma_2$, and $\beta_2 \in \mathbb{R}^d$, the FFN weights W_m and $W_n \in \mathbb{R}^{d \times d}$, the bias b_m and $b_n \in \mathbb{R}^d$. h is the number of attention heads. The mask $M \in \mathbb{R}^{d \times d}$ is an all-zero matrix in

encrypts the features before the output linear layer of the preceding FFN block. After the feature is computed with this linear layer on the GPU, it re-enters the TEE, where it is decrypted. Following the decryption, the add-norm computation is completed. Finally, the output feature of the add-norm layer is permuted and returned. The overall authorization process is summarized in Algorithm 1, and the detailed descriptions are provided in the following subsections.

Algorithm 1 TEE Authorization Process

Require: $y, W_m, b_m, W'_n, b_n, \gamma'_2, \beta'_2, \pi, p$

Ensure: $z\pi$

- 1: Calculate with the input linear layer as Eq.(7). // GPU
 - 2: Encrypt feature by the one-time mask as Eq.(8). // TEE
 - 3: Calculate with the output linear as Eq.(10). // GPU
 - 4: Decrypt feature and permutation as Eq.(11). // TEE
 - 5: Calculate with the add-norm layer as Eq.(12). // TEE
 - 6: Get authorized feature z' (i.e., $z\pi$) as Eq.(12). // TEE
- return** $z\pi$
-

Encryption. At the beginning, the input linear layer of the FFN block receives y as input from the previous layer:

$$m = \text{ReLU}(yW_m + b_m). \quad (7)$$

Following this, before the output linear layer, the feature is encrypted using an OTP. Additionally, to protect this encryption process from input-output differencing, we introduce positional obfuscation by applying a permutation:

$$m' = m\pi + p\pi, \quad (8)$$

where p is the pad, a noise matrix of the same shape as m , and m' is the encrypted permuted feature. The principle of the one-time pad (OTP) [30] ensures that p is different each time, thus even for the same m , m' produced will differ. In this way, the OTP encryption (i.e., p) and the permutation (i.e., π) can conceal each other.

Output Linear Layer. The encrypted feature is going to be processed by the output linear layer of the FFN block. However, since m' is permuted, to ensure the correctness of computations, the parameters of the linear layer must be aligned in advance. Specifically, we apply a corresponding permutation to the output linear layer (W_n) before deployment. This preprocessing process is as follows:

$$W'_n = \pi^T W_n. \quad (9)$$

With the above preparation, during inference, the encrypted feature m' is transferred to GPUs and processed by the permuted output linear layer W'_n :

$$n' = m' \pi^T W'_n = (m\pi + p\pi) \pi^T W_n + b_n = n + pW_n. \quad (10)$$

Decryption. However, if the OTP noise (i.e., pW_n) is not eliminated, the network's functionality will be compromised. Specifically, the implementation of OTP must meet two requirements: 1) both the addition and removal of the pad must be concealed; 2) all computations that the encrypted features undergo before decryption must be linear. Therefore, to meet the above requirements, n' is transferred to the TEE for decryption:

$$n'' = n' - pW_n = n. \quad (11)$$

Note that following prior work [37], computing pW_n can be conducted by the model provider or inside TEE in an offline phase. Both strategies do not increase the overhead of online inference or impede its efficiency [44].

Authorization. Lastly, the decrypted feature is processed by the add-norm layer and permuted to achieve authorization. To maintain security, the entire process is performed within the TEE. The steps are as follows:

$$z' = (\gamma_2 \odot \frac{n + y - \mu_{y+n}}{\sigma_{y+n}} + \beta_2) \pi = z\pi, \quad (12)$$

where z' (i.e., $z\pi$) is the authorized feature, which will be the input feature for the subsequent permuted transformer layer thus achieving authorized usage.

In conclusion, in the entire TEE authorization process, the TEE only needs to perform authorization once for each inference, thus the communication overhead is minimal (specifically, limiting TEE-GPU transfers to 5 rounds). Additionally, the authorization process requires the TEE to perform only lightweight computations, ensuring the computation overhead is minimal.

Security Analysis. Potential attackers might attempt to steal the locked model by the recovery of permuted parameters. However, it is impossible as the probability of guessing the correct π is $1/(d!)$. In practice, d is typically larger than 512, e.g., $d = 4096$ in LLaMA [36].

Another strategy for stealing is to crack (or simulate) the authorization process based on its overall functionality. Notably, CoreGuard employs the OTP to make any attempt at approximating the authorization process unfeasible. This is because, even with identical inputs, the TEE produces different outputs for each inference, as both p and pW_n vary with each inference. However, a sophisticated attacker might attempt to simulate the authorization process on a larger scale, e.g., attempting to map the relationship from the start (y) to the end ($z\pi$) to circumvent the OTP encryption. Nonetheless, it is also ineffective (as demonstrated in Section 4.2), since the permutation process is nonlinear, and even slight simulation errors can render the results unusable [8].

4 EXPERIMENTS

In this section, we perform extensive experiments to answer the following research questions (RQs):

RQ1: How does CoreGuard's security compare to other defenses, particularly in protecting the foundational capabilities of LLMs? **RQ2:** How does CoreGuard's computation and communication overhead compare to other defenses? **RQ3:** Does CoreGuard sacrifice the accuracy of the model?

4.1 Experimental Settings

Datasets. To evaluate CoreGuard's effectiveness, we assess it on four representative domain-specific tasks: GSM8k (mathematics) [6], Spider (code generation) [43], PubMedQA (medical question answering) [13], and SQuAD (reading comprehension) [29].

Models. We choose four representative LLMs for validation. Two of them are specifically designed for on-device use: Qwen2-0.5B-Instruct [42], Gamma2-2B-it [35]. The other two are larger models: ChatGLM3-6B-32k [8] and LLaMA3-8B-Instruct [36].

Metric. For all tasks, we use accuracy (ACC) as the metric. Specifically, for GSM8k, an output is considered correct when the final answer matches the actual result. For PubMedQA, a 3-class classification task, a prediction is deemed correct if it matches the true label. For Spider, we follow the prior work [5, 17] and assess whether the generated query matches the reference query. For SQuAD, we follow the prior work [41] and align the answer with the reference word for word. To evaluate execution overhead, we follow prior work to use Floating Point Operations (*FLOPs*) as metric [11, 34].

Implementation Details. We conduct our experiments using the *Huggingface transformers library*¹. For optimization, we follow the previous work [40] to use the AdamW [15] optimizer and a linear learning rate scheduler. Following previous work [40], we report results of the runs that achieve the highest performance, consistent with real-world practices prioritizing optimal model.

Baselines. To evaluate our proposed methods, we establish comprehensive baselines. These baselines consist of ideal cases (i.e., lower bound and upper bound) and representative defenses, which are categorized based on their underlying principles (i.e., TPTE, PPTE, and PSP): ① **Lower bound:** (i) No-shield, where the adversary can directly obtain the unprotected model. ② **Upper bound:** (i) Black-box, we consider a black-box setting, where attackers can only identify the architecture of the locked model, which is the strongest protection. ③ **TPTE solutions** (only protect task-related parameters): (i) No Privacy Left Outside (NPLO) [44]. ④ **PPTE solutions** (protect a subset of the mode): (i) DarkneTZ [22]; (ii) SOTER [31]; (iii) Serdab [9]; (iv) Our proposed baseline, Direct TEE Execution (DTE), directly executes the later half of the transformer layers via TEE. ⑤ **PSP solutions** (protect parameters through shuffling): (i) ShadowNet [33]; (ii) TransLinkGuard (TLG) [18].

To adapt these methods to transformer models, we rigorously configure each solution based on its papers. Specifically, for SOTER, TEE randomly shields 20% layers. For Serdab, the TEE shields the first transformer layers. ShadowNet obfuscates and offloads all the linear transformation layers. For DarkneTZ, the last transformer layer and subsequent parts are put into TEE.

Model Stealing Attack. We consider model stealing attacks as a key security challenge of existing protection solutions. Following prior work [44], we leverage the attack implementation specifically designed for edge-deployed models.

The attack consists of two phases: *foundational capabilities stealing* (P_1) and *task-specific adaptation* (P_2). In P_1 , to exploit the foundational capabilities of the locked model (M_{loc}), the attack begins by inferring the architecture of M_{loc} through its exposed parts. Following this, a replica model, M_{rep} , is constructed with the same architecture as M_{loc} . Finally, the attacker transports M_{loc} 's exposed weights to the corresponding parts of M_{rep} . In P_2 , the attacker attempts to fine-tune M_{rep} for their tasks. To this end, one potential approach is to train M_{rep} with the training dataset the attacker possesses. Specifically, we assume the attacker has access to the entire training dataset, making this scenario more challenging than previous works[44], which assume attackers have access to only a small portion (e.g., 1%) of the data. In the training, we mainly

consider a more comprehensive and effective method, namely full-parameter training (FFT). However, to ensure comprehensiveness, we also consider other training settings, such as LoRA.

4.2 Security Evaluation

Security against Unauthorized Usage. In this subsection, we assess the security of CoreGuard against unauthorized usage. We first evaluate CoreGuard's ability to prevent direct unauthorized inference. Then, we assess its security against MS attacks.

Table 1 reports the results: in all cases, the unauthorized inference ("Unau") accuracy is 0%, demonstrating CoreGuard's strong resistance to unauthorized inference. In terms of MS attacks, the security of CoreGuard is comparable to the *upper bound*, indicating that attackers cannot misuse the foundational capabilities of the protected model for downstream tasks. Specifically, CoreGuard's relative accuracy is 1.17× compared to the black-box baseline, while the other defense, such as DarkneTZ, shows a much higher relative value of 8.43×. Notably, the relative accuracy of CoreGuard (1.17×) is similar to that of DTE (1.18×), which achieves protection by placing the equivalent layers into the TEE. This suggests that permutation is an effective parameter protection method, which offers a similar protection to the strongest protection (i.e., direct parameter protection by TEE). Additionally, TLG (1.07×) and ShadowNet (1.09×) also demonstrate black-box-level security. In contrast, the TPTE solution, NPLO (9.59×), offers no defense (no-shield is 9.58×).

Security under Other Attack Settings. In this subsection, we assess the effectiveness of CoreGuard under various attack settings. Specifically, first, prior evaluations focus on FFT as the training method for MS. To test CoreGuard's security under different training methods, we assess its security against MS using LoRA, a most commonly used LLM fine-tuning approach. Second, previous evaluations take base models as the deployed model, but in real-world scenarios, LLMs may also be task-customized, which could affect the defense. Therefore, we assess CoreGuard's performance in such cases, where the customized task may differ from or align with the attacker's target. Third, while CoreGuard's security is close to the upper bound with a full training set, attackers may sometimes only have access to a small portion of data. To verify whether it can still approach the upper bound in such cases, where the upper bound is also lower, we assess the defense with varying training data, ranging from 1% to 100%. As shown in Figure 3, we report the defense performance under various attack settings on Qwen2-0.5B, and CoreGuard consistently ensures the model's security across various settings. The attack accuracies stay close to black-box protection and significantly lower than no-shield cases, regardless of whether the original task matches the target task, the proportion of data the attacker possesses, or the training method used.

Security against Permutation Matrix Simulation Attack. In this subsection, we assess the security of CoreGuard against attackers familiar with the CoreGuard's mechanism and implement attacks accordingly. Specifically, the core of authorization involves the permutation matrix (i.e., π), which the TEE protects. Therefore, an attacker might first attempt to simulate π by initializing a substitute permutation matrix with the same shape and training it based on the TEE's input and output to approximate the true π . Then, the

¹<https://huggingface.co/docs/transformers/index>

Table 1: Security assessment of CoreGuard in preventing unauthorized direct inference and model stealing attack. For *direct inference*, we report the authorized (“Auth”) and unauthorized (“Unau”) usage accuracies. For *model stealing attacks*, we report the attack accuracies, lower attack accuracies indicate stronger defense. The last row reports the average attack accuracies of each defense relative to the baseline black-box solutions. The column representing CoreGuard (“Ours”) is highlighted in bold.

		Direct Inference		Model Stealing Attack									
		Unau	Auth	No-shield	NPLO	Serdab	DarkneTZ	SOTER	TLG	ShadowNet	DTE	Ours	Black-box
Qwen2-0.5B	GSM8k	0.00%	15.51%	21.53%	20.92%	14.96%	16.81%	12.50%	1.43%	1.34%	2.36%	2.41%	1.29%
	Spider	0.00%	5.56%	28.48%	30.28%	23.90%	26.01%	21.52%	3.31%	3.67%	3.92%	3.79%	3.81%
	PubMedQA	0.00%	15.50%	58.00%	56.50%	49.00%	51.50%	47.00%	3.50%	4.50%	5.50%	6.00%	5.00%
	SQuAD	0.00%	16.50%	30.54%	32.33%	28.42%	29.89%	26.34%	6.81%	5.93%	4.42%	7.35%	5.66%
Gamma2-2B	GSM8k	0.00%	30.10%	40.94%	40.50%	35.18%	37.07%	32.67%	4.58%	10.81%	4.56%	3.91%	1.74%
	Spider	0.00%	3.52%	39.15%	38.83%	24.80%	23.29%	12.81%	0.00%	0.00%	0.00%	0.00%	0.00%
	PubMedQA	0.00%	10.50%	69.50%	69.00%	55.50%	60.00%	55.50%	10.50%	7.00%	9.50%	12.00%	6.50%
	SQuAD	0.00%	43.21%	63.96%	63.94%	60.82%	61.02%	57.87%	7.91%	6.71%	7.51%	7.81%	8.81%
ChatGLM3-6B	GSM8k	0.00%	37.13%	55.95%	55.07%	53.67%	54.91%	54.55%	2.84%	0.43%	0.93%	1.04%	0.23%
	Spider	0.00%	5.15%	35.81%	37.03%	32.25%	33.81%	33.22%	6.19%	8.31%	8.44%	7.37%	7.91%
	PubMedQA	0.00%	46.00%	71.00%	70.00%	63.00%	65.50%	60.50%	10.00%	12.00%	12.00%	12.50%	12.00%
	SQuAD	0.00%	62.11%	68.13%	68.21%	66.28%	63.91%	62.61%	8.61%	9.56%	9.42%	8.98%	9.15%
LLaMA3-8B	GSM8k	0.00%	33.11%	53.07%	53.83%	47.79%	51.31%	49.75%	5.61%	4.15%	6.09%	6.22%	4.05%
	Spider	0.00%	10.67%	40.04%	41.73%	38.27%	38.14%	36.63%	0.00%	0.57%	1.40%	1.08%	0.22%
	PubMedQA	0.00%	29.00%	77.00%	77.00%	72.50%	72.50%	68.00%	9.50%	10.00%	12.50%	11.00%	10.50%
	SQuAD	0.00%	73.02%	75.91%	75.20%	67.92%	73.81%	69.12%	11.94%	9.64%	10.48%	10.11%	9.71%
Average		-	-	9.58×	9.59×	8.48×	8.43×	8.09×	1.07×	1.09×	1.18×	1.17×	1.00×

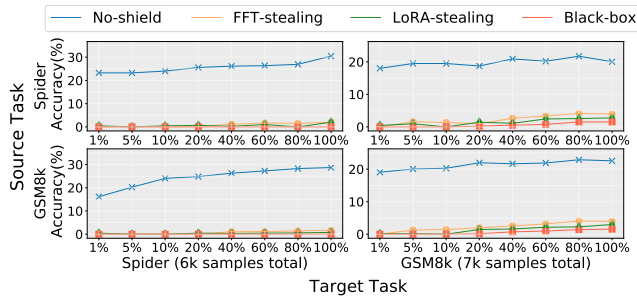


Figure 3: CoreGuard’s Defense Effectiveness Against Model Stealing Across Various Attack Settings.

attacker uses the simulated π to mimic the TEE’s authorization and fine-tunes the model on their task to complete the attack.

Table 2: Security evaluation of CoreGuard against permutation matrix simulation attack (*simulation*).

		No-Shield	Simulation	Black-box
Qwen2	GSM8k	21.53%	0.00%	1.29%
	PubMedQA	58.00%	3.50%	5.00%
Gamma2	Spider	39.15%	0.00%	0.00%
	SQuAD	63.96%	0.00%	8.81%
ChatGLM3	GSM8k	55.95%	0.00%	0.23%
	PubMedQA	71.00%	1.00%	12.00%
LLaMA3	Spider	40.04%	0.00%	0.22%
	SQuAD	75.91%	3.18%	9.71%

The results are shown in Table 2; the attack is ineffective, even performing worse than the black-box baseline. The outstanding security is due to the targeted design. Specifically, the non-linear nature of the authorization process, which relies on π , significantly increases the difficulty of the simulation. Moreover, CoreGuard requires high precision in the authorization process, where even slight simulation errors can compromise model performance.

Security against Authorization Simulation Attack. Considering that precisely fitting π is a challenging task, we consider that attackers might attempt to extend their simulation to include adjacent layers or structures, potentially making the attack more feasible. Specifically, since the TEE and the FFN block jointly achieve the

authorization, they can be considered as a single unit, which the attacker might attempt to simulate directly. Therefore, the attacker could reconstruct an FFN block structure and train this new FFN block based on the input and output of the original TEE-authorized FFN block, thereby bypassing the TEE’s authorization.

Table 3: Security evaluation of CoreGuard against authorization simulation attack (*simulation*).

		No-Shield	Simulation	Black-box
Qwen2	GSM8k	21.53%	2.72%	1.29%
	PubMedQA	58.00%	7.00%	5.00%
Gamma2	Spider	39.15%	0.00%	0.00%
	SQuAD	63.96%	3.51%	8.81%
ChatGLM3	GSM8k	55.95%	0.00%	0.23%
	PubMedQA	71.00%	13.50%	12.00%
LLaMA3	Spider	40.04%	0.00%	0.22%
	SQuAD	75.91%	6.81%	9.71%

As shown in Table 3, the attack is ineffective. In all cases, the attack accuracy is similar between the simulation and the black-box baseline but significantly lower than the no-shield baseline. The outstanding defense effectiveness is due to the targeted design. Specifically, CoreGuard disrupts the alignment of the parameters before and after the authorization, making it highly challenging for attackers to simply adjust the FFN to recover the compatibility between the two sets of parameters.

Security under Different Authorization Position. The position of authorization is a hyper-parameter of CoreGuard, and its selection can influence the overall security. To identify the best authorization position, we examine how different authorization positions impact security. Specifically, we place the authorization before various transformer layers and evaluate their security based on model-stealing attacks.

As shown in Figure 4, the results demonstrate that placing the initial authorization point in the middle of the network is practical. Specifically, the model stealing accuracy is higher when the authorization is placed near the beginning or end of the network. Conversely, when the authorization is deployed within the central layers of the network, the model-stealing accuracy significantly decreases. This aligns with our expectations: applying authorization at the first layer means CoreGuard permutes nearly all the

Table 4: The results of additional overhead. For *execution overhead*, we present the original model’s FLOPs (“Original”), the additional overhead in TEE (FLOPs), and its proportion to the original model’s FLOPs (%FLOPs). For *transfer overhead*, we report the transfer volume (KB) and the number of transfers (rounds) between the TEE and GPU for each method.

Models	TEE Execution Overhead FLOPs/(%FLOPs)								TEE-GPU Transfer Overhead KB/rounds							
	Original	Serdab	DarkneTZ	SOTER	TLG	ShadowNet	DTE	Ours	Serdab	DarkneTZ	SOTER	TLG	ShadowNet	DTE	Ours	
Qwen2	1.27E+11	3.82E+09 (3.02%)	3.82E+09 (3.02%)	2.59E+10 (20.48%)	3.54E+07 (9.27e-01%)	3.67E+10 (28.97%)	4.58E+10 (36.23%)	1.47E+06 (1.17e-03%)	2.24E+02	1.12E+02	5.50E+04	1.42E+05	2.75E+05	2.24E+02	6.18E+03	
Gamma2	6.70E+11	1.99E+10 (2.98%)	1.99E+10 (2.98%)	1.44E+11 (21.52%)	7.67E+07 (3.85e-01%)	1.89E+11 (28.23%)	2.59E+11 (38.72%)	2.95E+06 (4.41e-04%)	5.76E+02	2.88E+02	1.30E+05	3.95E+05	6.49E+05	5.76E+02	1.58E+04	
ChatGLM3	1.53E+12	5.22E+10 (3.41%)	5.22E+10 (3.41%)	3.01E+11 (19.65%)	2.26E+08 (4.32e-01%)	4.86E+11 (31.75%)	7.31E+11 (47.77%)	8.06E+06 (5.27e-04%)	1.02E+03	5.12E+02	1.78E+05	5.91E+05	1.02E+06	1.02E+03	2.19E+04	
LLaMA3	1.92E+12	5.58E+10 (2.91%)	5.58E+10 (2.91%)	3.85E+11 (20.02%)	1.51E+08 (2.70e-01%)	5.03E+11 (26.15%)	8.94E+11 (46.50%)	4.72E+06 (2.46e-04%)	1.02E+03	5.12E+02	2.82E+05	6.36E+05	1.31E+06	1.02E+03	2.05E+04	

Table 5: The accuracy comparison between the original model (M_{ori}) and the CoreGuard-protected model (M_{loc}). The accuracy is presented in the form of M_{ori}/M_{loc} . Cells showing changes in accuracy are highlighted in bold.

	GSM8k	Spider	PubMedQA	SQuAD
Qwen2	15.51%/ 15.50%	5.56%/5.56%	15.50%/15.50%	16.50%/16.50%
Gamma2	30.10%/30.10%	3.51%/3.51%	10.50%/10.50%	43.21%/43.21%
ChatGLM3	37.13%/37.13%	5.15%/5.15%	46.00%/46.00%	62.11%/62.09%
LLaMA3	30.10%/30.10%	3.51%/3.51%	10.50%/10.50%	43.21%/43.21%

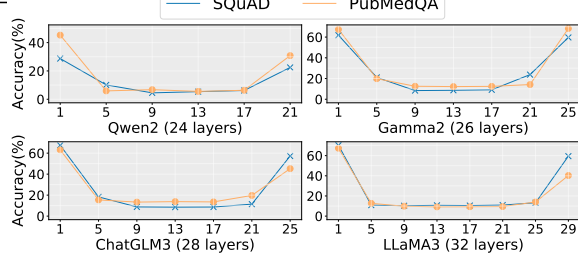


Figure 4: Impact of authorization position on security. Model-stealing accuracy is reported for different positions, with the total number of transformer layers indicated for each model.

transformer layers, which means the attacker only needs to recover the functionality of the first transformer layer. In contrast, placing authorization in the middle leaves at least half of the parameters unaligned, requiring the attacker to recover the functionality of at least half of the network’s parameters. Thus, placing the authorization in the central layers is an adequate strategy.

Answer to RQ1: CoreGuard achieves upper-bound security in protecting the LLMs under various attack assumptions, which benefit from our proposed permutation strategy that provides robust parameter protection.

4.3 Execution and Transfer Overhead

To answer RQ2, we measure both TEE execution and TEE-GPU transfer overheads to provide a comprehensive evaluation of CoreGuard’s efficiency in terms of computation and communication. Specifically, we take an example length of 128 as input and report the TEE execution and data transfer overhead to generate a single token. We do not present the results of NPLO, which has proved ineffective in protecting the backbone (in Section 4.2). As shown in Table 4, CoreGuard achieves a smaller TEE execution overhead than other defenses. Specifically, the additional overhead caused by CoreGuard is less than 0.1% for all cases. On the contrary, the TEE execution overhead of other defenses ranges from 3.0337% to

38.0071%, i.e., CoreGuard takes 30× less computation overhead. For transfer overhead, while both ShadowNet and TLG provide black-box level protection, CoreGuard’s transfer overhead is nearly two orders of magnitude lower due to its communication-friendly authorization design. Specifically, as mentioned in Section 3.3, CoreGuard requires only a single authorization, which is optimal, limiting the transfer rounds to 5. In contrast, ShadowNet requires two transfers per linear layer, resulting in an unacceptable overhead.

Answer to RQ2: Among protections that achieve black-box level protection, CoreGuard’s computation and communication overheads are significantly lower than the others.

4.4 Accuracy Loss

To answer RQ3, we compare the accuracy between the unprotected model M_{ori} and the CoreGuard-protected model M_{loc} . The result is shown in Table 5. As demonstrated, the impact of CoreGuard on accuracy is minimal. Specifically, there is no difference in accuracy between M_{ori} and M_{loc} in most cases. However, for some specific cases, accuracy slightly fluctuates (highlighted in bold). For example, with LLaMA3 on PubMedQA, accuracy decreases slightly by 0.5%. Despite these fluctuations, interestingly, we observe a 0.02% improvement on GSM8k. Therefore, we consider that the minor accuracy fluctuations are caused by data precision limitations (e.g., floating-point rounding errors or slight variations during inference) rather than by the defense itself, which is inevitable.

Answer to RQ3: While significantly outperforming existing defenses in terms of both security and efficiency, CoreGuard maintains the model’s accuracy without compromise.

5 LIMITATION AND DISCUSSION

Real-World Efficiency Evaluation. Although platform-irrelevant metrics (e.g., FLOPs and KB) demonstrate that CoreGuard incurs minimal additional overhead, the diversity of hardware and variations in testing environments prevent us from systematically evaluating the actual overhead. Future research could conduct extensive performance tests across various hardware platforms and environments to ensure a comprehensive efficiency analysis.

Side Channel Attacks. CoreGuard uses TEEs as a security measure, which makes it vulnerable to side-channel attacks [1, 32, 38]. However, various defense methods have emerged in recent years to mitigate the risk of side-channel leaks, and both these software [16, 19] and hardware-based [7, 39] defense solutions can be integrated into our approach. For software-based defense, CoreGuard

uses TEE only for basic matrix operations (e.g., matrix permutation and addition). For hardware-based defense, CoreGuard does not require modifications to hardware, allowing physical defense measures to be compatible.

TEE in GPUs. Recent work explored implementing a trusted environment directly inside GPUs [12, 21, 23]. However, such solutions are primarily designed for server centers and require high-end hardware [24, 45]. In contrast, CoreGuard is designed to be compatible with commodity hardware, ensuring its broad applicability.

6 CONCLUSIONS

In this paper, we introduce a protection method named CoreGuard for edge-deployed LLMs. CoreGuard utilizes a permutation strategy to safeguard these models, thus achieving black-box-level protection. Importantly, to reduce transfer overhead during inference, CoreGuard proposes an authorization propagation protocol, thus only a single authorization is required to authorize the entire model, which is optimal. The comprehensive experiments indicate that CoreGuard exhibits exceptional security and efficiency compared to the existing approaches without accuracy loss. In conclusion, CoreGuard is an effective solution to protect the edge-deployed proprietary LLMs, providing model owners with the means to safeguard their valuable intellectual property.

REFERENCES

- [1] AKM Mubashwir Alam and Keke Chen. 2023. Making your program oblivious: a comparative study for side-channel-safe confidential computing. In *2023 IEEE 16th International Conference on Cloud Computing (CLOUD)*. IEEE, 282–289.
- [2] Tiago Alves. 2004. Trustzone: Integrated hardware and software security. *Information Quarterly* 3 (2004), 18–24.
- [3] Apple Inc. 2024. Deploying Transformers on the Apple Neural Engine. <https://machinelearning.apple.com/research/neural-engine-transformers>. Accessed: [2024.08.05].
- [4] Tom Brown, Benjamin Mann, Nick Ryder, Melanie Subbiah, Jared D Kaplan, Prafulla Dhariwal, Arvind Neelakantan, Pranav Shyam, Girish Sastry, Amanda Askell, et al. 2020. Language models are few-shot learners. *Advances in neural information processing systems* 33 (2020), 1877–1901.
- [5] Ruisheng Cao, Lu Chen, Zhi Chen, Yanbin Zhao, Su Zhu, and Kai Yu. 2021. LGEQL: Line Graph Enhanced Text-to-SQL Model with Mixed Local and Non-Local Relations. In *Proceedings of the 59th Annual Meeting of the Association for Computational Linguistics and the 11th International Joint Conference on Natural Language Processing (Volume 1: Long Papers)*. 2541–2555.
- [6] Karl Cobbe, Vineet Kosaraju, Mohammad Bavarian, Mark Chen, Heewoo Jun, Lukasz Kaiser, Matthias Plappert, Jerry Tworek, Jacob Hilton, Reiichiro Nakano, et al. 2021. Training verifiers to solve math word problems. *arXiv preprint arXiv:2110.14168* (2021).
- [7] Ghada Dessouky, Tommaso Frassetto, and Ahmad-Reza Sadeghi. 2020. {HybCache}: Hybrid {Side-Channel-Resilient} caches for trusted execution environments. In *29th USENIX Security Symposium (USENIX Security 20)*. 451–468.
- [8] Zhengxiao Du, Yujie Qian, Xiao Liu, Ming Ding, Jiezhong Qiu, Zhilin Yang, and Jie Tang. 2021. Glm: General language model pretraining with autoregressive blank infilling. *arXiv preprint arXiv:2103.10360* (2021).
- [9] Tarek Elgamal and Klara Nahrstedt. 2020. Serdab: An IoT framework for partitioning neural networks computation across multiple enclaves. In *2020 20th IEEE/ACM International Symposium on Cluster, Cloud and Internet Computing (CCGRID)*. IEEE, 519–528.
- [10] Google. 2023. Gemini. <https://blog.google/technology/ai/google-gemini-ai/>. Accessed: [2024.03.12].
- [11] Kaiming He, Xiangyu Zhang, Shaoqing Ren, and Jian Sun. 2016. Deep residual learning for image recognition. In *Proceedings of the IEEE conference on computer vision and pattern recognition*. 770–778.
- [12] Weizhe Hua, Muhammad Umar, Zhiru Zhang, and G Edward Suh. 2022. Guardnn: secure accelerator architecture for privacy-preserving deep learning. In *Proceedings of the 59th ACM/IEEE Design Automation Conference*. 349–354.
- [13] Qiao Jin, Bhuwan Dhingra, Zhengping Liu, William W Cohen, and Xinghua Lu. 2019. Pubmedqa: A dataset for biomedical research question answering. *arXiv preprint arXiv:1909.06146* (2019).
- [14] David Kaplan, Jeremy Powell, and Tom Woller. 2016. AMD memory encryption. *White paper* 13 (2016).
- [15] Diederik P Kingma. 2014. Adam: A method for stochastic optimization. *arXiv preprint arXiv:1412.6980* (2014).
- [16] Paul Leignac, Olivier Potin, Jean-Baptiste Rigaud, Jean-Max Dutertre, and Simon Pontié. 2019. Comparison of side-channel leakage on Rich and Trusted Execution Environments. In *Proceedings of the Sixth Workshop on Cryptography and Security in Computing Systems*. 19–22.
- [17] Jinyang Li, Binyuan Hui, Reynold Cheng, Bowen Qin, Chenhao Ma, Nan Huo, Fei Huang, Wenyu Du, Luo Si, and Yongbin Li. 2023. Graphix-t5: Mixing pre-trained transformers with graph-aware layers for text-to-sql parsing. In *Proceedings of the AAAI Conference on Artificial Intelligence*, Vol. 37. 13076–13084.
- [18] Qinfeng Li, Zhiqiang Shen, Zhenghan Qin, Yangfan Xie, Xuhong Zhang, Tianyu Du, and Jianwei Yin. 2024. TransLinkGuard: Safeguarding Transformer Models Against Model Stealing in Edge Deployment. *arXiv preprint arXiv:2404.11121* (2024).
- [19] Tengchao Ma, Changqiao Xu, Qingzhao An, Xiaohui Kuang, Lujie Zhong, and Luigi Alfredo Grieco. 2022. A Proactive Defense Strategy Against SGX Side-channel Attacks via self-checking DRL in the Cloud. In *ICC 2022-IEEE International Conference on Communications*. IEEE, 4174–4179.
- [20] Frank McKeen, Ilya Alexandrovich, Alex Berenzon, Carlos V Rozas, Hisham Shafi, Vedvyas Shanbhogue, and Uday R Savagaonkar. 2013. Innovative instructions and software model for isolated execution. *Hasp@ isca* 10, 1 (2013).
- [21] Microsoft Azure. 2024. <https://azure.microsoft.com/en-us/blog/azure-confidential-computing-with-nvidia-gpus-for-trustworthy-ai/>. <https://azure.microsoft.com/en-us/blog/azure-confidential-computing-with-nvidia-gpus-for-trustworthy-ai/>. Accessed: [2024.10.11].
- [22] Fan Mo, Ali Shahin Shamsabadi, Kleomenis Katevas, Soteris Demetriou, Ilias Leontiadis, Andrea Cavallaro, and Hamed Haddadi. 2020. Darknetz: towards model privacy at the edge using trusted execution environments. In *Proceedings of the 18th International Conference on Mobile Systems, Applications, and Services*. 161–174.
- [23] NVIDIA. 2024. NVIDIA Confidential Computing. <https://www.nvidia.com/en-us/data-center/solutions/confidential-computing/>. Accessed: [2024.10.11].
- [24] NVIDIA. 2024. NVIDIA H100 Tensor Core GPU. <https://www.nvidia.com/en-us/data-center/h100/>. Accessed: [2024.3.18].
- [25] OpenAI. 2023. GPT-4. <https://openai.com/gpt-4>. Accessed: [2023.11.17].
- [26] Tribhuvanesh Orekondy, Bernt Schiele, and Mario Fritz. 2019. Knockoff nets: Stealing functionality of black-box models. In *Proceedings of the IEEE/CVF conference on computer vision and pattern recognition*. 4954–4963.
- [27] Soham Pal, Yash Gupta, Aditya Shukla, Aditya Kanade, Shirish Shevade, and Vinod Ganapathy. 2020. Activethief: Model extraction using active learning and unannotated public data. In *Proceedings of the AAAI Conference on Artificial Intelligence*, Vol. 34. 865–872.
- [28] Alec Radford, Jeffrey Wu, Rewon Child, David Luan, Dario Amodei, Ilya Sutskever, et al. 2019. Language models are unsupervised multitask learners. *OpenAI blog* 1, 8 (2019), 9.
- [29] Pranav Rajpurkar, Jian Zhang, Konstantin Lopyrev, and Percy Liang. 2016. Squad: 100,000+ questions for machine comprehension of text. *arXiv preprint arXiv:1606.05250* (2016).
- [30] Claude E Shannon. 1949. Communication theory of secrecy systems. *The Bell system technical journal* 28, 4 (1949), 656–715.
- [31] Tianxiang Shen, Ji Qi, Jianyu Jiang, Xian Wang, Siyuan Wen, Xusheng Chen, Shixiong Zhao, Sen Wang, Li Chen, Xiaopu Luo, et al. 2022. {SOTER}: Guarding Black-box Inference for General Neural Networks at the Edge. In *2022 USENIX Annual Technical Conference (USENIX ATC 22)*. 723–738.
- [32] Petr Socha, Vojtěch Miškovský, and Martin Novotný. 2022. A comprehensive survey on the non-invasive passive side-channel analysis. *Sensors* 22, 21 (2022), 8096.
- [33] Zhichuang Sun, Ruimin Sun, Changming Liu, Amrita Roy Chowdhury, Long Lu, and Somesh Jha. 2023. Shadownet: A secure and efficient on-device model inference system for convolutional neural networks. In *2023 IEEE Symposium on Security and Privacy (SP)*. IEEE, 1596–1612.
- [34] Mingxing Tan and Quoc Le. 2019. Efficientnet: Rethinking model scaling for convolutional neural networks. In *International conference on machine learning*. PMLR, 6105–6114.
- [35] Gemma Team, Thomas Mesnard, Cassidy Hardin, Robert Dadashi, Surya Bhupatiraju, Shreya Pathak, Laurent Sifre, Morgane Rivière, Mihir Sanjay Kale, Juliette Love, et al. 2024. Gemma: Open models based on gemini research and technology. *arXiv preprint arXiv:2403.08295* (2024).
- [36] Hugo Touvron, Louis Martin, Kevin Stone, Peter Albert, Amjad Almahairi, Yasmine Babaei, Nikolay Bashlykov, Soumya Batra, Prajwal Bhargava, Shruti Bhosale, et al. 2023. Llama 2: Open foundation and fine-tuned chat models. *arXiv preprint arXiv:2307.09288* (2023).
- [37] Florian Tramer and Dan Boneh. 2018. Slalom: Fast, verifiable and private execution of neural networks in trusted hardware. *arXiv preprint arXiv:1806.03287* (2018).

- [38] Jo Van Bulck, Nico Weichbrodt, Rüdiger Kapitza, Frank Piessens, and Raoul Strackx. 2017. Telling your secrets without page faults: Stealthy page {Table-Based} attacks on enclaved execution. In *26th USENIX Security Symposium (USENIX Security 17)*. 1041–1056.
- [39] Wubing Wang, Mengyuan Li, Yinqian Zhang, and Zhiqiang Lin. 2023. PwrLeak: Exploiting Power Reporting Interface for Side-Channel Attacks on AMD SEV. In *International Conference on Detection of Intrusions and Malware, and Vulnerability Assessment*. Springer, 46–66.
- [40] Guangxuan Xiao, Ji Lin, and Song Han. 2023. Offsite-tuning: Transfer learning without full model. *arXiv preprint arXiv:2302.04870* (2023).
- [41] Ikuya Yamada, Akari Asai, Hiroyuki Shindo, Hideaki Takeda, and Yuji Matsumoto. 2020. LUKE: Deep Contextualized Entity Representations with Entity-aware Self-attention. In *Proceedings of the 2020 Conference on Empirical Methods in Natural Language Processing (EMNLP)*. 6442–6454.
- [42] An Yang, Baosong Yang, Binyuan Hui, Bo Zheng, Bowen Yu, Chang Zhou, Chengpeng Li, Chengyuan Li, Dayiheng Liu, Fei Huang, et al. 2024. Qwen2 technical report. *arXiv preprint arXiv:2407.10671* (2024).
- [43] Tao Yu, Rui Zhang, Kai Yang, Michihiro Yasunaga, Dongxu Wang, Zifan Li, James Ma, Irene Li, Qingning Yao, Shanelle Roman, et al. 2018. Spider: A large-scale human-labeled dataset for complex and cross-domain semantic parsing and text-to-sql task. *arXiv preprint arXiv:1809.08887* (2018).
- [44] Ziqi Zhang, Chen Gong, Yifeng Cai, Yuanyuan Yuan, Bingyan Liu, Ding Li, Yao Guo, and Xiangqun Chen. 2023. No Privacy Left Outside: On the (In-) Security of TEE-Shielded DNN Partition for On-Device ML. In *2024 IEEE Symposium on Security and Privacy (SP)*. IEEE Computer Society, 52–52.
- [45] Jianwei Zhu, Hang Yin, and Shunfan Zhou. 2024. Confidential Computing on nVIDIA H100 GPU: A Performance Benchmark Study. *arXiv preprint arXiv:2409.03992* (2024).